Axial Impact Collapse Analysis of Spot Welded Hat Shaped Section Members

Cheon Seok Cha, Jong Yup Kang
Department of Mechanical Design Engineering Graduate School, Chosun University
In Young Yang*
School of Mechanical Engineering, Chosun University

The widely used spot welded sections of automobiles(hat and double hat shaped section members) absorb most of the energy in a front-end collision. The sections were tested with respect to axial static(10 mm/min) and quasi-static(1000 mm/min) loads. Based on these test results, specimens with various thicknesses, width ratios and spot weld pitches on the flange were tested at high impact velocity(7.19 m/sec and 7.94 m/sec) which simulates an actual car crash. Characteristics of collapse have been reviewed and structures for optimal energy absorbing capacity is suggested.

Key Words : Spot Welded Sections, Hat and Double Hat Shaped Section Members, Front-End Collision, Characteristics of Collapse

1. Introduction

The purpose of automobile design is to satisfy the standards and the requirements for general performance; the feeling of stability, calmness, firm handling and pleasantness. The safety capacity to protect the passengers in a car accident shall be affected by the conditions of collision, the structural integrity and protective equipment for passengers. The front-end collisions including the inclined collision amount to about 70 percent of all accidents. Thus, attention to safety capacity has increasingly been focused on the front-end collisions in recent years(Ishikawa, 1985; Haug et al., 1996).

The front-head is the structure needed to support the engine and suspension systems, to contain other attachments and to absorb the impact energy in a front-end collision. Many vehicles have been designed to absorb it through plastic deformation using hat and double hat shaped section members in a front-end collision. Sufficiently absorbed in the front parts, the collision energy does not reach the passengers by decelerating their speed against a wheel or structure(Pritz, 1983; Janssen, 1987; Jost, 1996). Simultaneously, the frame gets less damaged.

Above all, it is also important to understand the characteristics of energy absorption and the collapse by plastic deformation on a simple structure which endures a massive collision(Mahmood et al., 1981; Abramowicz et al., 1986; Li et al., 1990; Krauss et al., 1994; Avalle et al., 1997; Singace, 1999). However, it is very difficult to theoretically analyze the impact behavior because side members experience nonlinear behaviors including great amounts of geometrical deformation and plastic deformation.

Previous studies on the collapse characteristics of spot welded structures have been mainly static collapse tests and were performed to theoretically analyze the mean collapse load assuming the spot welded structure as being seamless(Wallentowitz, 1995; White et al., 1999; White et al., 1999).

* Corresponding Author,
E-mail : iyyang@mail.chosun.ac.kr
TEL : +82-62-230-6748 ; **FAX** : +82-62-230-7170
School of Mechanical Engineering, Chosun University, 375 Seosuk-dong, Dong-gu, Kwangju 501-759, Korea.
(Manuscript **Received** April 27, 2000; **Revised** November 10, 2000)

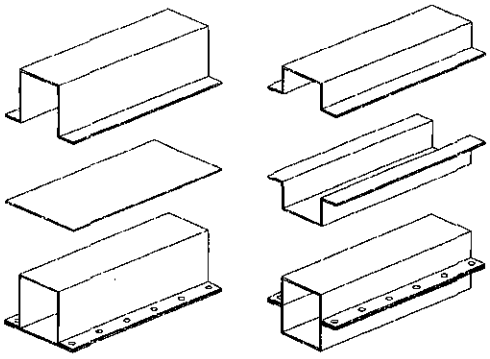

(a) Hat shaped section member (b) Double hat shaped section member

Fig. 1 Configuration of the specimens

Theoretical analysis is not easily derived because the member is not closed except for the areas of the spot welded points between the hat shaped section and the plane. It is not easy to find previous studies exhibiting the optimum conditions of the structure considering the relationship between load and deformation on high speed impact and changable spot weld pitch on the flanges.

The static(10 mm/min) and quasi-static(1000 mm/min) axial collapse experiments were implemented on the spot welded section members of automobiles(hat and double hat shaped sections). Based on the test results, specimens with various thicknesses, width ratios and spot weld pitches on the flanges were tested with high impact velocities(7.19 m/sec and 7.94 m/sec.) which simulates an actual car collision. Characteristics of impact collapse have been reviewed and a structure with an optimal energy absorbing capacity has been suggested.

2. Specimens

The specimens, hat and double hat shaped section members, were manufactured by welding the two parts as shown in Fig. 1 using SCP1, cold rolled sheet widely used for these structures. The spot welding was carried out under the condition of 220 voltage, 85 ampere and 1.5 seconds for all the specimens.

The hat and double hat shaped section members with thicknesses of 0.78 mm and 0.95 mm, width ratios of 30×30 mm, 33×27 mm and 36×24 mm, and 12 mm width flange were selected. Considering the theoretical folding width of 22 mm(Mahmood et al., 1981), three types of spot weld pitch were decided; 18.3 mm, 22 mm and 27.5 mm.

Table 1 Material constant of specimens

Specimen Thickness [mm]	Yield Strength [kgf/mm²]	Tensile Strength [kgf/mm²]	Elongation [%]
0.78	17.0	31.5	46.4
0.95	18.5	30.9	45.6

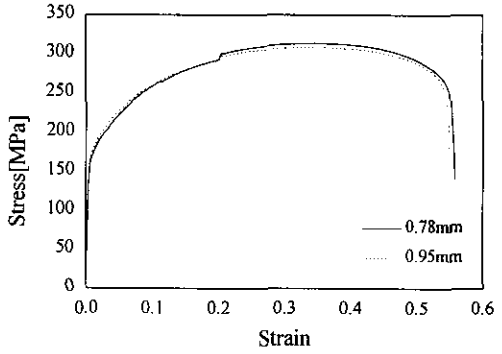

Fig. 2 Relationship between stress and strain from axial tensile test

Figure 2 is the stress-deformation diagram acquired from KS B 0802 tensile test. Table 1 shows the material constants of specimen and table 2 gives the definition of specimens.

3. Apparatus and Method

3.1 Axial static and quasi-static collapse tests

The static(10 mm/min) and quasi-static(1000 mm/min) axial collapse tests were implemented for various thicknesses, width ratios and spot weld pitches on the flanges for the hat shaped and double hat shaped section members, using UTM. By doing several preliminary tests, the specimens progressively collapsed to 70 mm of 120 mm in order not to be affected by the end effects, and the repetitive and agreeable test results were derived.

Figure 3 is the load and displacement curve of the static test on the hat shaped section members.

Table 2 Definition of the specimens

H(D)	T(000)	W(X, Y)	E(F, G)	S(Q, I_1, I_2)
Type H : Hat Shaped D : Double hat Shaped				
	Thickness 078 : 0.78mm 095 : 0.95mm			
		Width ratio(R=*b*/*h*) W : 30×30mm (1) X : 33×27mm (1.22) Y : 36×24mm (1.5)		
			Spot weld pitch E : 18.3mm F : 22mm G : 27.5mm	
				Load S : Static(10mm/min) Q : Quasi-static(1000mm/min) I_1 : Impact(7.19m/sec) I_2 : *Impact*(7.94m/sec)

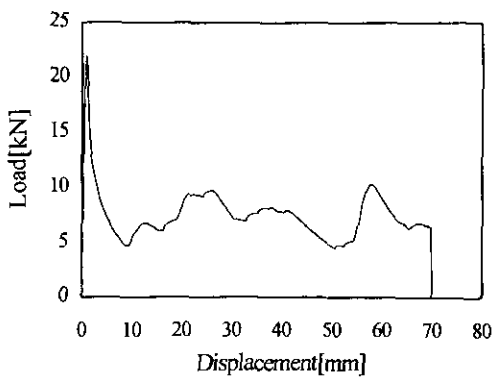

Fig. 3 Relationship between load and displacement, H078WFS

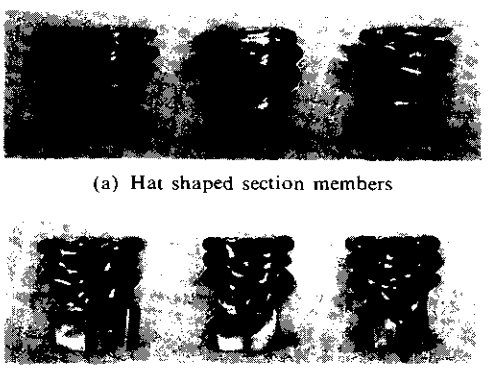

(a) Hat shaped section members

(b) Double hat shaped section members

Fig. 4 Profiles of specimens, static

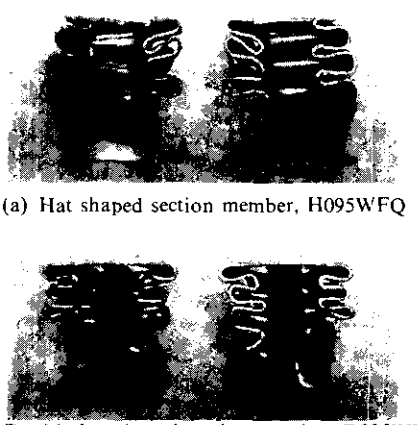

(a) Hat shaped section member, H095WFQ

(b) Double hat shaped section member, D095WFQ

Fig. 5 Cross section of collapsed specimens

As seen in Fig. 3 the absorbed energy is the inside area of the load-displacement curve. It is calculated by integrating the load and displacement diagram with Eq. (1), and each mean collapse load is acquired by dividing the absorbed energy into the displacement.

$$E_a = \int_{l_0}^{l} P dl \tag{1}$$

where E_a is the absorbed energy in the specimen and P is the collapse load.

The hat shaped section specimens of 30×30 mm, 33×27 mm, 34×26 mm, thickness of 0.95 mm, and spot weld pitch of 22 mm are shown in

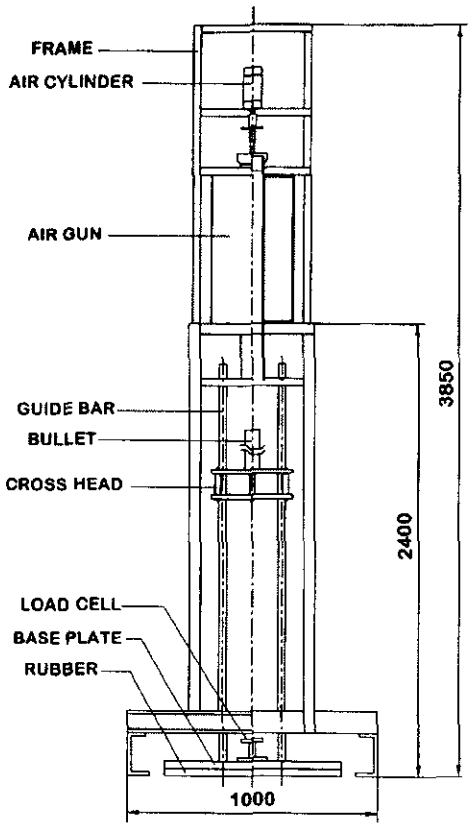

Fig. 6 Impact testing setup

Fig. 4(a), and the double hat shaped section specimens are shown in Fig. 4(b). The collapsed specimens are cut as shown in Fig. 5.

3.2 Axial impact collapse tests

The axial impact collapse test device using compressed air is presented in Fig. 6, and the system diagram is shown Fig. 7.

The test device consists of an air pressure accelerator, a cross head, a load cell, base plate, an anti-vibration rubber, an air cylinder, guide bars and frames. The cross head which is accelerated by the compressed air and guided by the four guide bars drops and collides with the load cell. These four guide bars are designed to protect two stories cross head from colliding off-center with the test specimen.

The cross head strikes the specimen and is a two story structure of which two mild steel plates(thickness of upper plate 18 mm, thickness

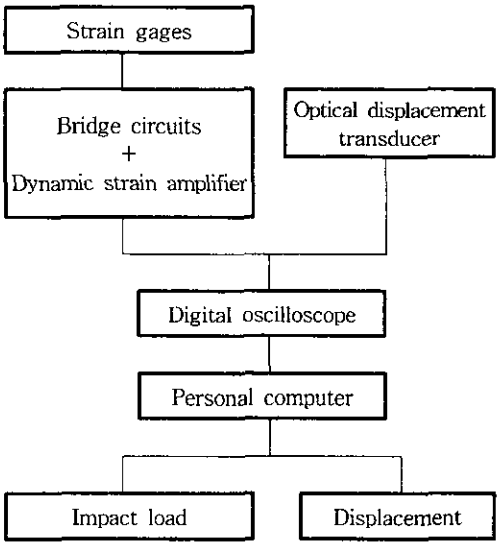

Fig. 7 Diagram of measurement system

of lower plate 23 mm, side length 320 mm) are connected with four posts. The plate has a hole at each corner to lead the four guide bars. The cross head weighs 40 kilogram. On its front side, a target is placed to measure the displacement, and on the opposite side a barrier is used to check the velocity.

The load cell is composed of two mild steel circle plates are connected by a round column. Specimens are put on the upper plate and the lower plate has three holes to be fixed on the base. Two semiconductor strain gages(KYOWA, KSP-2-120 E4) are symmetrically placed on both sides of the load cell. The load cell was designed to remove the bending effect.

In the tests, the impact loads were obtained by converting the electrical resistance variations of semiconductor strain gage into loads. In collision, the resistance variation of semiconductor strain gage going through the shield line and bridge box, is fed into a dynamic strain amplifier which converts the signal into variation of voltage. The signals are finally amplified.

Deformation on a specimen is measured by using an Optical Deformation System(ZIMMER OHG Co.) which captures the movement of target on the cross head.

The impact velocity was measured by a laser system before the cross head collided with the

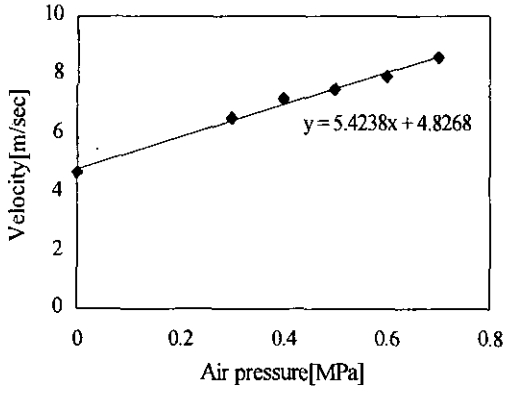

Fig. 8 Relation between air pressures and velocities

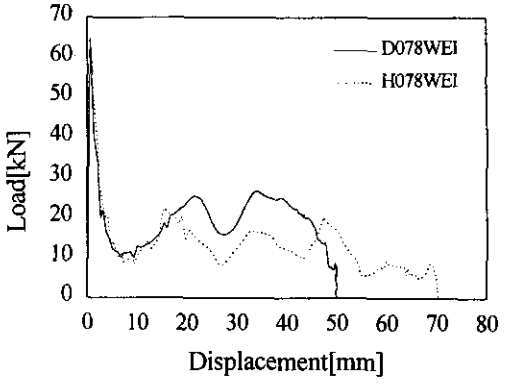

Fig. 9 Relationship between load and displacement

specimen. The relationship between the air pressure on the impact test device and the impact velocity is shown in Fig. 8. Two types of velocity were selected, 7.19 m/sec at 0.4 MPa and 7.94 m/sec at 0.6 MPa. The value of impact energy is similar to that given by Eq. (2): 1034J at 7.19 m/sec and 1260J at 7.94 m/sec.

$$E_I=\frac{1}{2}mv^2 \tag{2}$$

where m is the mass of cross head and v is the impact collapse velocity. It is considered that about 96 percent of the impact energy is consumed to deform the specimen during the collision and about 4 percent is dissipated into the repulsive energy, fraction energy, and sliding energy.

A load-displacement curve which shows the collapse history was obtained by eliminating the time axis from the measured time-load and time-displacement curves. Based on the load-displacement curve, absorbed energy(E_a), total absorbed energy(E_L), mean collapse load(P_{mean}), maximum collapse load($P_{max.}$) and deformed length(S) were derived. The absorption characteristics of each specimens were studied, especially because all the specimen did not collapse equally in length though the cross head imposed the same energy under same condition. It is assumed that specimens collapse as much as the total length of 120mm in order to obtain the total absorbed energy, which is E_L given as below.

$$E_L=E_aJ \tag{3}$$

(a) H078WFI$_1$ (b) D078WFI$_1$ (c) H095WFI$_1$ (d) D095WFI$_1$

Fig. 10 Profiles of collapsed specimens

where $J(=L/S)$ is the inverse stroke efficiency, S is the deformed length and L is the total length.

Figure 9 is the load-displacement diagram of hat and double hat shaped section members with width ratio of 30×30 mm and thickness of 0.78 mm which were acquired from the impact test(impact velocities of 7.19 m/sec and impact energy of 1034J). The solid line is for the double hat shaped section member and the broken line is for the hat shaped section member. Figure 10 presents the collapsed specimens which were collapsed at a velocity of 7.19 m/sec and imposed collapse energy of 1034J.

From the left shows the hat shaped section of thickness 0.78 mm-collapsed length; 76 mm of 120 mm, double hat shaped section of thickness 0.78 mm-collapsed length; 54 mm of 120 mm, hat shaped section of thickness 0.95 mm-collapsed length; 52 mm of 120 mm and double hat shaped section of thickness 0.95 mm-collapsed length; 40 mm of 120 mm are presented.

4. Results and Discussion

4.1 The collapse characteristics of hat shaped section members

Absorbed energy E_a, total absorbed energy E_L, mean collapse load P_{mean}, maximum collapse load $P_{max.}$ and deformed length S have been derived and collapse modes have been considered for three different types of velocities, static, quasi-static and impacts.

The box shaped section member is a seamless section, but the hat shaped section member consists of two parts, a ㄷ-type section and a plane, which are joined by spot welding. The hat shaped section member has a different collapse mode from that of the box shaped section member, because it is only closed in the areas of the spot weld points.

The collapse mode of the box shaped section member is a symmetrical accordion mode. On the other hand, as shown in Fig. 5(a), the hat shaped section member undergoes parallel mode. Since the buckling load of the plane section is lower than that of the ㄷ-shaped section, buckling in the plane leads to the collapse in the hat shaped section member. The spot weld pitch plays a important role in deciding the deformation mode throughout the hat shaped section because the spot weld restricts the plane by support of ㄷ-type section.

Tables 3 and 4 compare the averages of absorbed energies, total absorbed energies, mean collapse loads, maximum collapse loads and deformations among the static, quasi-static and impact collapse tests for various velocities, width ratios, and spot weld pitches on flanges.

Considering the values in Table 3 with respect to shifts of velocities and width ratio, the higher total absorption energy and mean collapse loads are presented in the case of higher width ratio under static and quasi-static loads, but vague

Table 3 Collapse test results for hat shaped section members with width ratios and velocities

Spec.	E_a[J]	E_L[J]	P_{mean}[kN]	$P_{max.}$[kN]	S[mm]
H078WFS	526.53	902.62	7.52	21.04	70
H078WFQ	676.03	1158.91	9.66	32.47	70
H078WFI$_1$	995.42	1571.72	13.10	61.86	76
H078XFS	513.04	879.50	7.33	20.05	70
H078XFQ	636.90	1091.83	9.10	30.46	70
H078XFI$_1$	1005.79	1588.09	13.23	63.42	76
H078YFS	577.52	990.03	8.25	20.09	70
H078YFQ	709.81	1216.82	10.14	30.11	70
H078YFI$_1$	1016.74	1564.22	13.04	62.18	78
H095WFS	778.67	1334.86	11.13	28.01	70
H095WFQ	845.46	1449.36	12.08	38.71	70
H095WFI$_1$	1012.56	2336.68	19.47	79.70	52
H095WFI$_2$	1218.61	2031.02	16.93	82.16	72
H095XFS	787.68	1350.31	11.25	28.72	70
H095XFQ	1008.27	1728.46	14.40	38.37	70
H095XFI$_1$	1004.00	2151.43	17.93	75.67	56
H095XFI$_2$	1203.28	2123.44	17.70	81.23	68
H095YFS	835.52	1432.32	11.94	28.64	70
H095YFQ	1018.05	1745.23	14.54	37.05	70
H095YFI$_1$	1019.09	2145.45	17.88	78.30	57

Table 4 Collapse test results for hat shaped section members with spot weld pitches on the flanges and velocities

Spec.	E_a[J]	E_L[J]	P_{mean}[kN]	$P_{max.}$[kN]	S[mm]
H078WES	561.91	963.27	8.03	22.66	70
H078WEQ	697.90	1196.41	9.97	32.91	70
H078WEI$_1$	1007.09	1678.48	13.99	64.81	72
H078WFS	526.53	902.62	7.52	21.04	70
H078WFQ	673.03	1153.77	9.66	32.47	70
H078WFI$_1$	995.42	1571.72	13.10	61.86	76
H078WGS	515.62	883.92	7.37	19.21	70
H078WGQ	650.19	1114.61	9.29	30.57	70
H078WGI$_1$	994.38	1529.82	12.75	62.46	78

under impact loads. This is mainly caused by the fact that the width of the plane becomes broad and interference between the plane and the ㄷ-type section occurs as width ratio increases. Also, the deformation mode due to change in width ratio was influenced by the ㄷ-type section member in the static and quasi-static tests. However in the impact tests plastic deformation influences it more than the ㄷ-type section, because the collapse occurs in an instant due to plastic deformation during the impact.

As the velocity increases, total absorbed energy, mean collapse load and maximum collapse load increase. However, the total absorbed energy and mean collapse load decrease more at 7.94 m/sec than at 7.19 m/sec. It is believed that the energy absorption characteristics dramatically decrease beyond a certain velocity by plastic deformation in a spot welded specimen.

In comparison between the shifts of velocities and that of spot weld in Table 4, the total absorbed energy and mean collapse load increases, as spot weld pitch gets smaller under all the loads: static, quasi-static and impact loads. The maximum collapse load increases at higher velocity, but it does not correlate with variations of the width ratio and spot weld pitch of the flanges. The maximum collapse load is proportional to the area and is affected by section types.

4.2 The collapse characteristics of double hat shaped section members

The double hat shaped section member is assumed to be close to the seamless section member similar to the hat shaped section member. As shown in Fig. 5(b), the double hat shaped section member undergoes unstable symmetric deformaton mode.

The deformation mode of the double hat shaped section member different from that of the hat shaped section member is developed by plastic deformation. Though it starts to collapse due to plastic deformation, it has high capacity for total absorbed energy and mean collapse load due to interference between the foldings of the flanges. This means that the double hat shaped section member has more absorption capacity than the hat shaped section member in high speed collision, if the progressive folding occurs continuously.

The absorbed energy, total absorbed energy, mean collapse load, maximum collapse loads and deformation from the static, quasi-static and impact collapse tests are compared in Tables 5 and 6 for various velocities, width ratios and spot weld pitches on the flanges.

These tables indicate that the total absorbed energy and mean collapse load increase in all three kinds of tests, static, quasi-static and impact, as the width ratio increases.

As the spot weld pitches on the flanges decrease, the total absorbed energy and mean collapse load under static, quasi-static and impact loads increase. Especially, noteworthy is the fact that the values of the impact load are conspicuously different from those under static

Table 5 Collapse test results for double hat shaped section members with width ratios and velocities

Spec.	E_a[J]	E_L[J]	P_{mean}[kN]	$P_{max.}$[kN]	S[mm]
D078WFS	828.32	1419.98	11.83	24.22	70
D078WFQ	978.98	1679.97	13.99	33.76	70
D078WFI$_1$	1004.75	2232.78	18.61	68.10	54
D078XFS	810.25	1389.00	11.58	23.42	70
D078XFQ	958.41	1642.99	13.69	30.56	70
D078XFI$_1$	1013.37	2251.93	18.77	63.16	54
D078YFS	850.00	1457.14	12.14	23.54	70
D078YFQ	1003.81	1720.82	14.34	31.93	70
D078YFI$_1$	981.75	2310.00	19.25	72.33	51
D095WFS	1205.85	2067.17	17.23	33.40	70
D095WFQ	1345.12	2305.92	19.22	41.22	70
D095WFI$_1$	996.93	2990.79	24.92	80.77	40
D095WFI$_2$	1156.16	2890.40	24.09	75.07	48
D095XFS	1220.32	2091.98	17.43	31.87	70
D095XFQ	1378.96	2363.94	19.70	41.19	70
D095XFI$_1$	985.95	3113.53	25.95	84.78	38
D095XFI$_2$	1153.51	2883.78	24.03	83.50	48
D095YFS	1263.73	2166.39	18.05	31.22	70
D095YFQ	1491.20	2556.34	21.30	40.97	70
D095YFI$_1$	989.62	3125.12	26.04	85.88	38
D095YFI$_2$	1212.09	2851.98	23.77	89.87	51

Table 6 Collapse test results for double hat shaped section members with spot weld pitches on the flanges and velocities

Spec.	E_a[J]	E_L[J]	P_{mean}[kN]	$P_{max.}$[kN]	S[mm]
D078WES	857.41	1469.85	12.25	25.03	70
D078WEQ	1008.72	1729.23	14.41	33.84	70
D078WEI$_1$	984.74	2317.04	19.31	66.13	51
D078WFS	828.32	1419.98	11.83	24.22	70
D078WFQ	978.98	1678.25	13.99	33.76	70
D078WFI$_1$	1004.75	2232.78	18.61	68.10	54
D078WGS	802.71	1376.07	11.47	23.79	70
D078WGQ	864.82	1482.55	12.35	33.08	70
D078WGI$_1$	984.64	1875.50	15.63	62.79	63

and quasi-static loads.

Figures 11 and 12 compare the mean collapse loads and maximum collapse loads for the hat and double hat shaped section members with thickness of 0.78 mm, as velocities and width ratios change, and Figs. 13 and 14 show the similar data for a thickness of 0.95 mm. In Figs. 15 and 16, mean collapse loads and maximum loads are compared for the hat shaped section members and the double hat shaped section members with thickness of 0.78 mm for various velocities and spot weld pitches on the flanges.

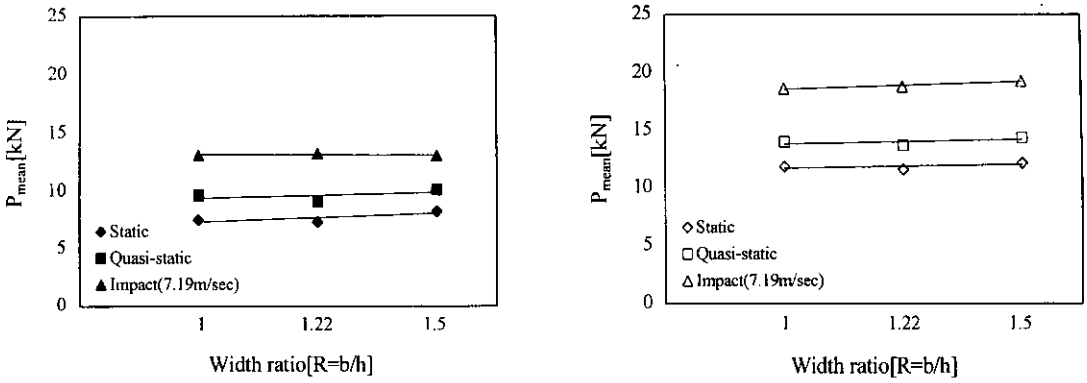

(a) Hat shaped section members (b) Double hat shaped section members

Fig. 11 Relationship between velocities-width ratios and mean collapse loads(Thickness 0.78 mm, Spot weld pitch 22 mm)

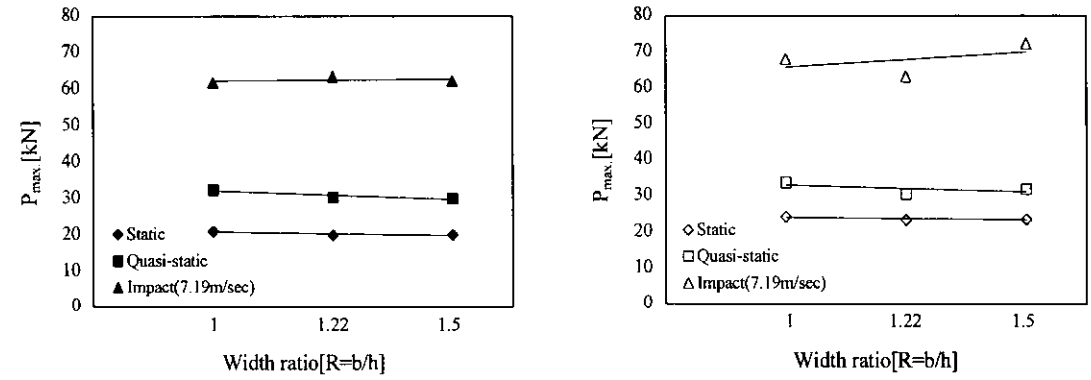

(a) Hat shaped section members (b) Double hat shaped section members

Fig. 12 Relationship between velocities-width ratios and maximum collapse loads(Thickness 0.78 mm, Spot weld pitch 22 mm)

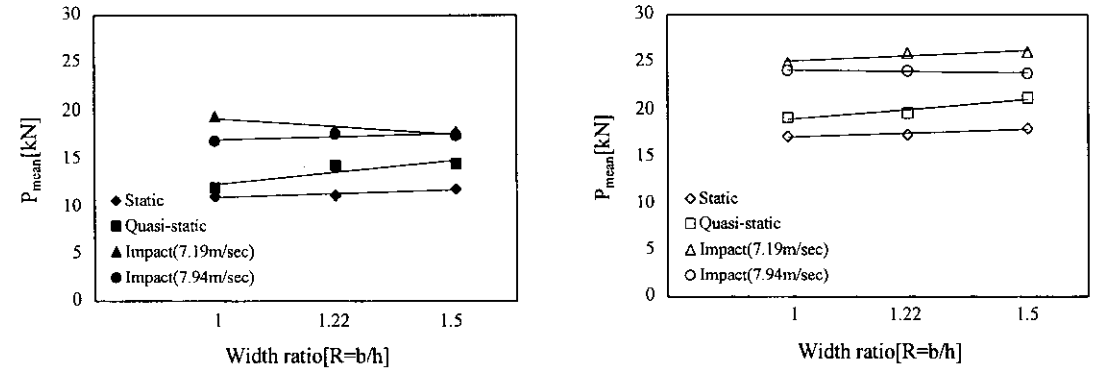

(a) Hat shaped section members (b) Double hat shaped section members

Fig. 13 Relationship between velocities-width ratios and mean collapse loads(Thickness 0.95 mm, Spot weld pitch 22 mm))

The total absorbed energy and mean collapse loads of the double hat shaped section member are about 55 percent higher for both static and quasi-static loads and about 39 percent higher for

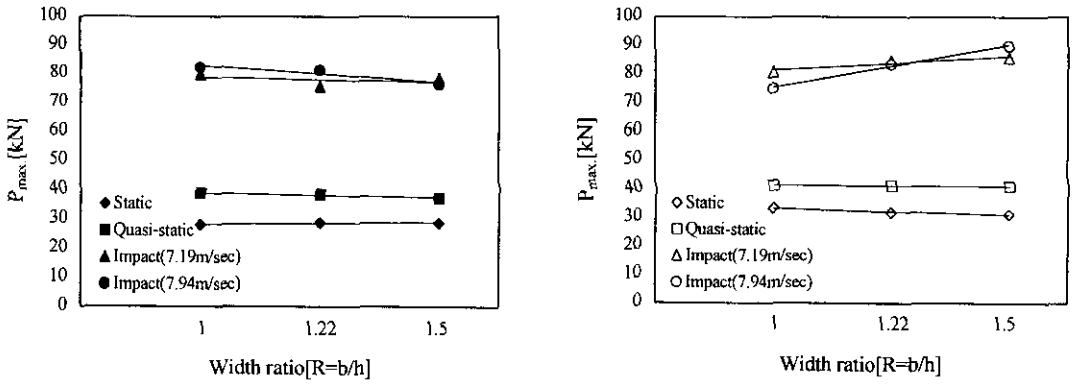

(a) Hat shaped section members (b) Double hat shaped section members

Fig. 14 Relationship between velocities-width ratios and maximum collapse loads(Thickness 0.95 mm, Spot weld pitch 22 mm)

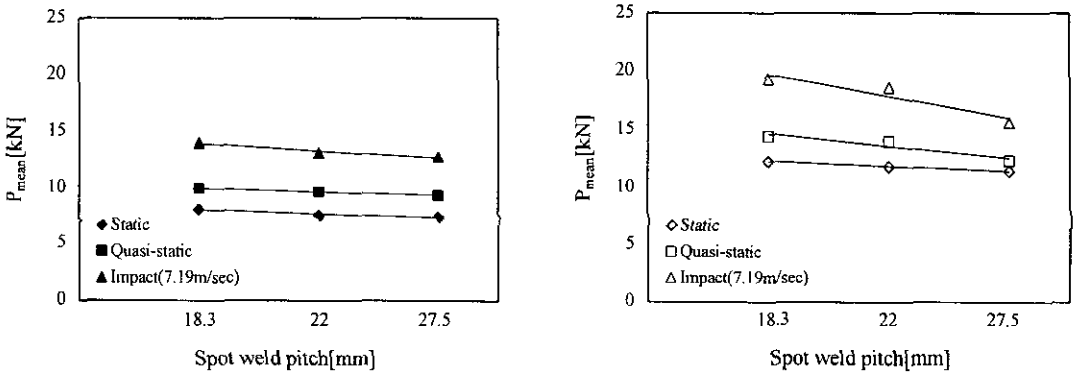

(a) Hat shaped section members (b) Double hat shaped section members

Fig. 15 Relationship between velocities-spot weld pitches and mean collapse loads(Thickness 0.78 mm, Width ratio 30×30 mm)

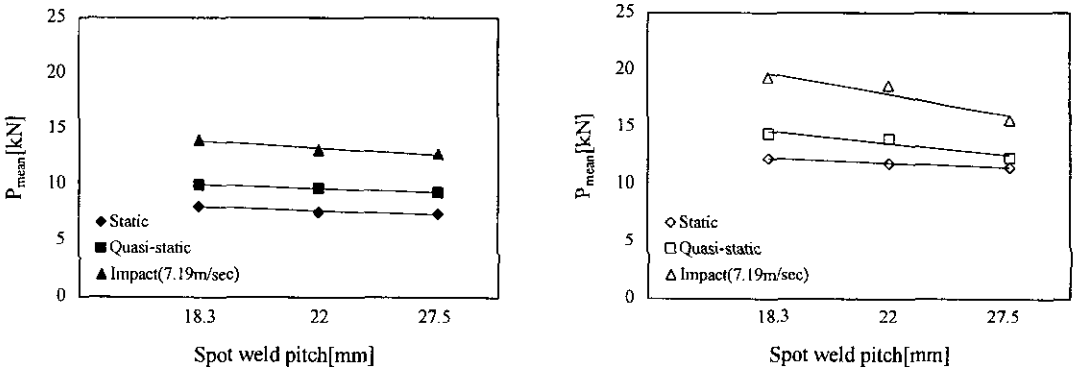

(a) Hat shaped section members (b) Double hat shaped section members

Fig. 16 Relationship between velocities-spot weld pitches and maximum collapse loads(Thickness 0.78 mm, Width ratio 30×30 mm)

impact load than those of hat shaped section member. Maximum collapse load is about 13 percent higher under static and quasi-static loads and about 6.5 percent higher under impact load.

Because 80 percent of the load during collapse is absorbed in the edges of a specimen (a hat shaped section member has four edges and a double hat shaped section member has eight edges) it is considered that absorbed energy, mean collapse load and maximum collapse load on impact load are higher than those for static and quasi-static loads.

As impact velocity increases, the difference among the values of absorbed energy, mean collapse load and maximum collapse load decreases. When collapse starts, the repulsive load rises sharply, and if the conditions around the collision are ideal, the stress would be everly distributed throughout the specimen. If the load increases more, buckling appears in the weak areas of the wall. Then, as the buckled wall fails the stress gets concentrated on the edges. Although buckling on the wall develops, the repulsive load increases during a short time without instant collapse of the edges. The repulsive load reaches the peak when the edges do not endure and start to collapse. As the impact velocity increases, the length of the first folding decreases. The difference among the maximum collapse loads with respect to the section types gets smaller, because the maximum collapse loads do not correlate with the variations of the width ratios and spot weld pitches at the same velocity. However, they are affected by shapes and the area of the section.

5. Conclusions

(1) The hat shaped section member undergoes parallel deformation mode. The deformation mode of the double hat shaped section member is almost the same as that of the box shaped section member. However, it undergoes unstable symmetric mode due to interference of the flanges.

(2) For static and quasi-static loads the total absorbed energy and mean collapse loads of the hat and double hat shaped section members are high with the largest width ratio, but there is no significant change under impact load.

(3) As spot weld pitch on the flanges decreases, the total absorbed energy and mean collapse loads increase under static, quasi-static and impact loads. Especially, under impact loads the values are conspicuously higher than those under static and quasi-static loads.

(4) As collapse velocity increases, the total absorbed energy, mean collapse loads and maximum collapse loads increase. However, the collapse characteristics show a drop at a certain velocity due to imperfection where the spot welded section member is not perfectly closed.

(5) The total absorbed energy and mean collapse loads of the double hat shaped section member are about 55% higher under static and quasi-static loads and about 39% higher under impact load than those of the hat shaped section member. The maximum collapse load is about 13% higher under static and quasi-static loads and about 6.5% higher under impact load. As collapse velocity increases, the difference among the values of the total absorbed energy, mean collapse load and maximum collapse load decreases.

Referances

Abramowicz, W. and Jones, N., 1986, "Dynamic Progressive Buckling of Circular and Square Tubes," *International Journal Impact Engineering*, Vol. 4, No. 4, pp. 243~270.

Avalle, M. and Belingardi, G., 1997, "Experimental Evaluation of the Strain Field History during Plastic Progressive Folding of Aluminium Circular Tubes," *International Journal of Mechanical Science*, Vol. 39, No. 5, pp. 575~583.

Haug, E., Clinckemaillie, J., Ni, X., Pickett, A. K. and Queckborner, T., 1996, "Recent Trends and Advances in Crash Simulation and Design of Vehicles," *Proceedings of the NATO-ASI*, July, pp. 343~359.

Ishikawa, H., 1985, "Computer Simulation of Automobile Collision, Reconstruction of Accidents," SAE Paper No. 851729.

Janssen, E. G., 1987, "Evaluation of Vehicle-cyclist Impacts through Dummy and Human Cadaver Tests," 11th ESV.

Kevin Jost., 1986, "Air Bag Technology Trends," Automotive Engineering, pp. 67~80.

Krauss, C. A. and Laananen, D. H., 1994, "A Parametric Study of Crush Initiators for a Thin-walled Tube," *International Journal of Vehicle Design*, Vol. 15, pp. 385~401.

Li, S. and Reid, S. R., 1990, "Relationship between the Elastic Bucking of Square Tubes and Rectangular Plates," *International Journal of Applied Mechanics*, Vol. 57, pp. 969~973.

Mahmood, H. F., and Paluszny, A., 1981, "Design of Thin Walled Columns for Crash Energy Management-Their Strength and Mode of Collapse," *Proc. 4rd Instructural Conference on Vehicle Structural Mechanics*, Nov. 18-20, Detoit, pp. 7~18.

Pritz, H. B., 1983, "Experimental Investigation of Pedestrian Head Impacts on Hood and Fenders of Production Vehicles," SAE Paper No. 830055.

Singace, A. A., 1999, "Axial Crushing Analysis of Tubes Deforming in the Multi-lobe Mode," *International Journal of Mechanical Science* 41, pp. 865~890.

Wallentowitz, H. and Adam, H., 1995, "Prediction the Crushworthiness of Vehicle Structures Made by Lightweight Design Materials and Innovative Joining Methods," *ASME*, AMD-Vol. 210/BED-Vol. 30, pp. 331~354.

White, M. D. and Jones, N., 1999, "Experimental Quasi-static Axial Crushing of Top-hat and Double-hat Thin-walled Sections," *International Journal of Mechanical Science*, 41, pp. 179~208.

White, M. D., Jones, N. and Abramowicz, W., 1999, "A Theoretical Analysis for the Quasi-static Axial Crushing of Top-hat and Double-hat Thin-walled Sections," *International Journal of Mechanical Sciences*, 41, pp. 209~233.